

3-Aryl Substituted Triazole Derivatives as New and Effective Corrosion Inhibitors for Mild Steel in Hydrochloric Acid Solution

M. A. Quraishi^{1*}, Sudheer¹, K. R. Ansari¹, Eno E. Ebenso²

¹ Department of Applied Chemistry, Indian Institute of Technology, (Banaras Hindu University) Varanasi -221 005, (India)

² Department of Chemistry, School of Mathematical and Physical Sciences, North-West University (Mafikeng Campus), Private Bag X2046, Mmabatho 2735, South Africa

*E-mail: maquraishi.apc@itbhu.ac.in; maquraishi@rediffmail.com

Received: 16 June 2012 / Accepted: 9 July 2012 / Published: 1 August 2012

The corrosion inhibition properties of three triazoles derivatives namely 4-amino-5-phenyl-4*H*-1, 2, 4,-triazole-3-thiol (APTT), 4-amino-5-(2-hydroxy) phenyl-4*H*-1, 2, 4,-triazole-3-thiol, (AHPTT), 4-amino-5-styryl-4*H*-1, 2, 4,-triazole-3-thiol, (ASTT) on mild steel corrosion in 1.0 M HCl solution was studied using electrochemical impedance spectroscopy (EIS), potentiodynamic polarization and weight loss methods. Potentiodynamic polarization study clearly revealed that the triazoles derivatives act as mixed type inhibitors. Adsorption of the inhibitors on the mild steel surface followed Langmuir adsorption isotherm. The values of free energy of adsorption (ΔG°_{ads}) indicated that adsorption of triazoles derivatives is a spontaneous process and they are adsorbed chemically as well as physically. The values of inhibition efficiency for all triazoles followed the order ASTT > AHPTT > APTT. The Styryl substituted triazole exhibited highest inhibition efficiency 95.2 % at concentration of 5.72×10^{-4} mol L⁻¹.

Keywords: Electrochemical; Corrosion inhibition; Acid solution; Adsorption

1. INTRODUCTION

The use of organic compounds as corrosion inhibitors is one of the most practical methods for prevention of metallic corrosion in acid medium [1, 2]. Heterocyclic organic compounds constituent a potential class of corrosion inhibitors they contain heteroatoms such as O, N, S, and π bonds in their molecules through which they are adsorbed on the metal surface [3, 6]. Corrosion protection prevents the waste of both resources and money during the industrial applications and extends the lifetime of

the equipments. Triazoles possess wide spectrum of activities ranging from anti-bacterial, anti-inflammatory, anticonvulsant, anti-neoplastic, [7-10]. A few triazoles have been reported as corrosion inhibitors in different corrosive environment [11-14].

In the present study, three triazoles namely 4-amino-5-phenyl-4*H*-1, 2, 4,-triazole-3-thiol (APTT), 4-amino-5-(2-hydroxy) phenyl-4*H*-1, 2, 4,-triazole-3-thiol, (AHPTT), 4-amino-5-styryl-4*H*-1, 2, 4,-triazole-3-thiol, (ASTT) are investigated for their inhibition action on corrosion of mild steel in 1.0 HCl. Electrochemical impedance spectroscopy (EIS), potentiodynamic polarization, linear polarization measurement and weight loss methods were used. The choice of triazoles as corrosion inhibitors is based on the following considerations. They are conveniently synthesized in high yield from commercially available raw materials. Triazoles molecules contain four nitrogen atoms one S atom πe^- and aromatic ring through which they can easily adsorbed on metal surface and bring about inhibition. Literature survey reveals that these compounds have not been used as corrosion inhibitors.

2. EXPERIMENTAL

2.1 Materials

The mild steel coupons of rectangular size ($2.5 \times 2.0 \times 0.025$) cm having the composition ; (wt %): C 0.17%; Mn 0.46%; Si 0.026%; Cr 0.050%; P 0.012%; Cu 0.135%; Al 0.023%; Ni 0.05%; and balance Fe were used for weight loss studies. Pretreatment of mild steel coupons included abrasion with emery paper as described previously [15]. Triazoles derivatives were prepared according to the literature [16]. The test solution 1.0 M HCl solution was prepared from analytical reagent. The molecular structure and IUPAC name of synthesized compounds are given in Fig. 1.

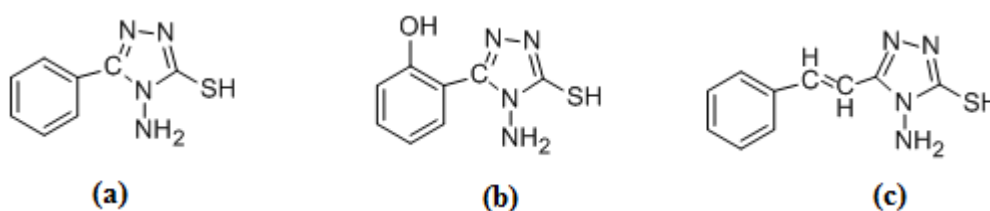


Figure 1. The molecular structure and IUPAC name of triazoles derivatives (a) 4-amino-5-phenyl-4*H*-1, 2, 4,-triazole-3-thiol (b) 4-amino-5-(2-hydroxy) phenyl-4*H*-1, 2, 4,-triazole-3-thiol (c) 4-amino-5-styryl-4*H*-1, 2, 4,-triazole-3-thiol

2.2 Procedures

2.2.1 Weight loss measurements

For weight loss experiments, clean weighed metal rectangular coupons were immersed in 100 ml of 1.0 M HCl solution in conical flasks for 3 h at 308 K temperature. These coupons were taken out, washed, dried, and weighed accurately with or without different concentration of triazoles

derivatives. Triplicate experiments were performed in weight loss test for each concentration of inhibitors and without inhibitors and average of weight loss is reported. The inhibition efficiency ($\eta_{\%}$) and surface coverage (θ) was determined by using following equation:

$$\theta = \frac{w_0 - w_i}{w_0} \quad (1)$$

$$\eta_{\%} = \frac{w_0 - w_i}{w_0} \times 100 \quad (2)$$

where w_0 and w_i is the weight loss value in absence and in the presence of inhibitor, respectively.

2.2.2 Electrochemical measurements

The electrochemical measurements were carried out using a Gamry Potentiostat/Galvanostat with a Gamry framework system based on ESA400. Gamry applications include software DC105 for corrosion, EIS300 for EIS measurements, and Echem Analyst version 5.50 software packages used for data fitting. These measurements were accomplished with a three electrodes cell assembly at constant temperature of 308 K. Mild steel coupons having exposed area 1.0×1.0 cm, was used as working platinum, and saturated calomel electrode were used as counter electrode, and reference electrode respectively. All potentials were measured versus SCE. All the impedance measurements were performed under a potentiodynamic condition from 100,000 Hz to 0.01 Hz with amplitude of 10 mV peak-to-peak. The polarization measurements were performed by changing the electrode potential automatically from -250 to +250mV vs. OCP at a scan rate of 1 mV s^{-1} . The linear Tafel segments of anodic and cathodic curves were extrapolated to the corrosion potential to obtain corrosion current densities (I_{corr}). The linear polarization study was carried out from cathodic potential of -20mV vs. OCP to an anodic potential of +20mV vs. OCP at a scan rate 0.125 mVs^{-1} to study the polarization resistance (R_p). The polarization resistance was calculated from the slope of curve in the vicinity of corrosion potential. Prior to the electrochemical measurements, the working electrode was immersed in 1.0 M HCl with and without addition of inhibitor for 30 minutes for stabilization of the OCP wrt SCE.

3 RESULTS AND DISCUSSIONS

3.1 Weight loss studies

3.1.1 Effect of inhibitor concentration

The corrosion rate (C_r) in ($\text{mg cm}^{-2} \text{ h}^{-1}$) was determined using the following equation:

$$C_r = \frac{w}{At} \quad (3)$$

where w is a weight loss of coupons mild steel (mg), A the area of the coupon (cm^2), t is the exposure time (h). The value of inhibition efficiency ($\eta_{\%}$) and corrosion rate (C_r) obtained from weight loss method at different concentrations in 1.0 M HCl at 308 K temperature are presented in Tables 1 and 2. From the Table 1 it is clear that increase of inhibitor concentrations caused a decrease in the weight loss as well as corrosion rate of mild steel.

3.1.2. Effect of temperature

In order to study the effect of temperature on the inhibition characteristic of triazoles derivatives, weight loss measurements were performed at different temperatures from 308 to 338 K in the absence and presence of $5.72 \times 10^{-4} \text{ mol L}^{-1}$ concentrations of triazoles for 3 h immersion time. The results are given in Table 2. It is seen that the inhibition efficiency decreased around 30 % in the presence of $5.72 \times 10^{-4} \text{ mol L}^{-1}$ concentration of triazoles at the studied temperature range which indicated desorption of inhibitor molecules to some extent with increasing temperature [17].

The activation energy (E_a) for the corrosion process in the absence and presence of the triazoles were evaluated from Arrhenius equation.

$$C_r = \lambda e^{-E_a/RT} \quad (4)$$

Table 1. Corrosion parameters obtained weight loss test for mild steel in 1.0 M HCl and containing various concentrations of triazoles at 308 K.

Inhibitors	Concentration (mol L ⁻¹)	Corrosion rate (mg cm ⁻² h ⁻¹)	Surface coverage (θ)	η (%)
1.0 M HCl	-	7.0	0.0	-
APTT	1.14×10^{-4}	2.20	0.686	68.6
	2.29×10^{-4}	1.83	0.738	73.8
	3.43×10^{-4}	1.36	0.805	80.5
	4.58×10^{-4}	0.86	0.876	87.6
	5.72×10^{-4}	0.63	0.910	91.0
AHPTT	1.14×10^{-4}	2.06	0.705	70.5
	2.29×10^{-4}	1.70	0.757	75.7
	3.43×10^{-4}	1.26	0.819	81.9
	4.58×10^{-4}	0.70	0.900	90.0
	5.72×10^{-4}	0.50	0.929	92.9
ASTT	1.14×10^{-4}	1.63	0.767	76.7
	2.29×10^{-4}	1.03	0.852	85.2
	3.43×10^{-4}	0.70	0.900	90.0
	4.58×10^{-4}	0.53	0.924	92.4
	5.72×10^{-4}	0.33	0.952	95.2

where E_a apparent activation energy, λ the pre-exponential factor, T absolute temperature, R is the universal gas constant. Taking the logarithm of the Arrhenius equation yields [18]:

$$\log C_r = -\frac{E_a}{2.303RT} + \log \lambda \quad (5)$$

The Arrhenius plots for mild steel immersed in 1.0 M HCl in absence and in the presence of different triazoles (APTT, AHPTT and ASTT) are shown in Fig. 2a. The value of activation energy (E_a) obtained from the slope of the line ($-E_a/2.303R$), are listed in Table 3. It is evident that E_a are higher for inhibited solutions than that for uninhibited solution. The higher values of E_a could be interpreted as physical adsorption. The triazoles molecules create a barrier to charge and mass transfer. The higher values of E_a in inhibited solution might also be correlated with the increased thickness of double [19].

Table 2. Parameters obtained from weight loss measurements of mild steel in 1.0 M HCl containing optimum concentration of triazoles at different temperatures.

Inhibitors	Temperature (K)	Corrosion rate ($\text{mg cm}^{-2} \text{h}^{-1}$)	η (%)
1.0 M HCl	308	7.00	-
	318	9.66	-
	328	14.60	-
	338	18.73	-
APTT	308	0.63	91.0
	318	1.50	84.5
	328	4.10	71.9
	338	7.30	60.9
AHPTT	308	0.50	92.9
	318	1.33	86.2
	328	3.83	73.7
	338	7.0	62.6
ASTT	308	0.33	95.2
	318	0.76	92.0
	328	2.96	79.6
	338	6.16	67.0

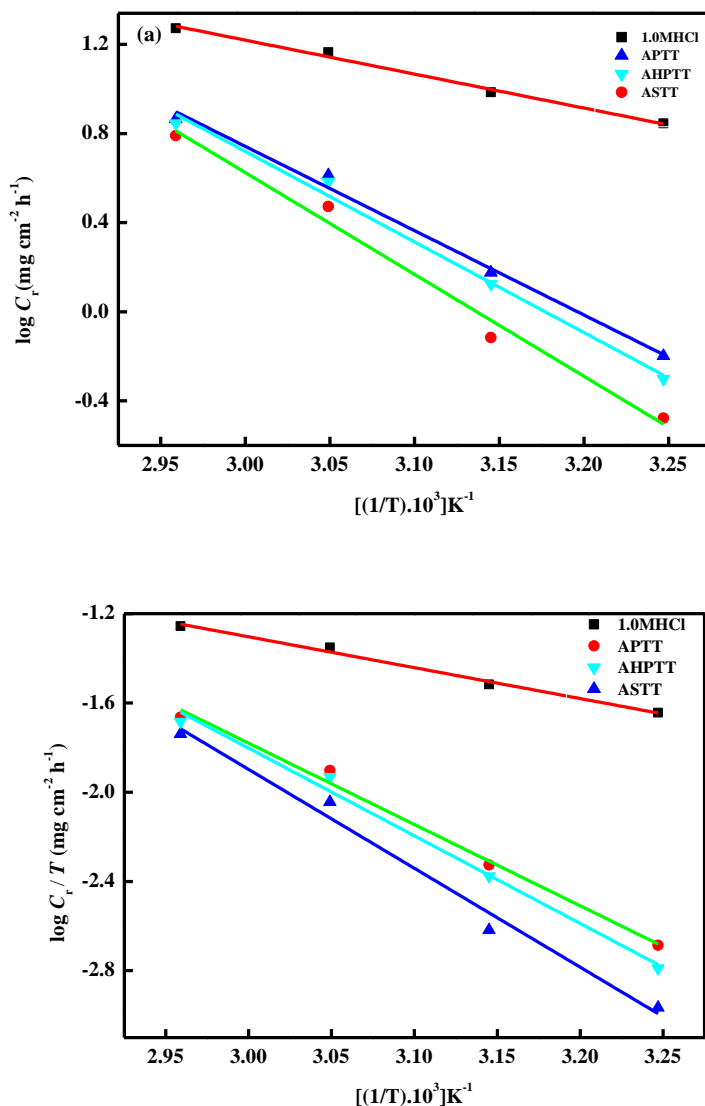


Figure 2. Arrhenius plots of: (a) $\log C_R$ vs. $1,000 / T$; (b) $\log (C_R / T)$ vs. $1,000 / T$ for the mild steel in 1.0 M HCl solution in the absence and presence of $(5.72 \times 10^{-4} \text{ mol L}^{-1})$ of APTT, AHPTT and ASTT.

To calculate enthalpy and entropy of activation for corrosion process transition state Eq. (6) was used [20]

$$C_r = \frac{RT}{Nh} \exp\left(-\frac{\Delta H^*}{RT}\right) \exp\left(\frac{\Delta S^*}{R}\right) \tag{6}$$

where h is the Planck's constant, N is the Avogadro's number, ΔS^* is the entropy of activation and ΔH^* is the enthalpy of activation. Fig. 2b, showed the plot of $\log C_r/T$ against $1/T$. The plots obtained are straight lines and the values of ΔH^* are calculated from their gradient ($\Delta H^* = -\text{slope}/2.303R$) and ΔS^* from intercept [$\log(R/Nh) + (\Delta S^*/2.303R)$]. The calculated data listed in Table

3. The positive signs of ΔH^* reflect the endothermic nature of mild steel dissolution process in the presence of triazoles. The values of ΔS^* are higher for inhibited solutions than that for the uninhibited solution suggesting an increase in randomness on going from reactants to the activated complex. The increase in values of entropy by the adsorption of triazoles molecules on metal surface from the acid solution could be regarded as quasi-substitution between the triazoles in the aqueous phase and H_2O molecules on electrode surface. In such condition, the adsorption of triazoles molecules was followed by desorption of H_2O molecules from the electrode surface. Thus increase in entropy of activation is attributed to solvent (H_2O) entropy [21, 22].

Table. 3. Thermodynamic activation parameters for copper in 1.0 M HCl in absence and presence of optimum concentration ($5.72 \times 10^{-4} \text{ mol L}^{-1}$) of APTT, AHPTT and ASTT.

Inhibitors	E_a (kJ mol ⁻¹)	ΔH^* (kJ mol ⁻¹)	ΔS^* (J mol ⁻¹ K ⁻¹)
1.0 M HCl	29.17	26.48	-143.09
APTT	72.45	69.78	-22.38
AHPTT	77.87	75.19	-6.54
ASTT	87.53	84.85	20.61

3.2 Adsorption isotherm

The most frequently used isotherms include: Langmuir, Frumkin, and Temkin isotherm. The adsorption isotherms provide information about interaction energy between inhibitors and metal surface. Langmuir adsorption isotherm was found to be best fit. Surface coverage (θ), the concentration (C_{inh}) of the inhibitor in the bulk of the solution is related to the following equation [23]:

$$\theta = \frac{K_{\text{ads}} C_{\text{inh}}}{1 + K_{\text{ads}} C_{\text{inh}}} \quad (7)$$

where K_{ads} is the equilibrium constant for the adsorption/desorption process and C_{inh} is the inhibitor concentration in mol L^{-1} . This equation can be rearranged to

$$\frac{C_{\text{inh}}}{\theta} = \frac{1}{K_{\text{ads}}} + C_{\text{inh}} \quad (8)$$

Plots of C_{inh}/θ as function of C_{inh} yielded a straight line as shown in Fig. 3. The obtained plots of the triazoles are almost linear with correlation coefficient (R^2) ranging from 0.9914-0.9994 for Langmuir adsorption isotherm. K_{ads} can be calculated from the intercepts of the straight lines in Fig. 3.

Free Energy of adsorption (ΔG_{ads}^0), is related to the adsorption constant (K_{ads}) by the following equation:

$$K_{\text{ads}} = \frac{1}{55.5} \exp\left(\frac{-\Delta G_{\text{ads}}^0}{RT}\right) \quad (9)$$

Logarithmic form of Eq. (9),

$$\ln K_{\text{ads}} = \frac{-\Delta G_{\text{ads}}^0}{RT} + \ln \frac{1}{55.5} \quad (10)$$

where 55.5 is the concentration of water in solution in mol L⁻¹ and R is the universal gas constant [24]. The values of K_{ads} and ΔG_{ads}^0 are given in Table 4. The negative values of ΔG_{ads}^0 ensure the spontaneity of the adsorption process and stability of the adsorbed layer on the steel surface. Generally, values of ΔG_{ads}^0 , around -20 kJ mol⁻¹ or lower are consistent with the electrostatic interaction between the charged molecules and charge metal, such as physisorption.

Table 4. Calculated parameters for Langmuir adsorption isotherm for APTT, AHPTT and ASTT on the mild steel in 1.0 M HCl by polarization and impedance methods.

Inhibitors	K _{ads} (M ⁻¹ x 10 ⁴)	ΔG _{ads} ^o (kJ mol ⁻¹)
APTT	1.43	-34.79
AHPTT	1.48	-34.88
ASTT	2.49	-36.22

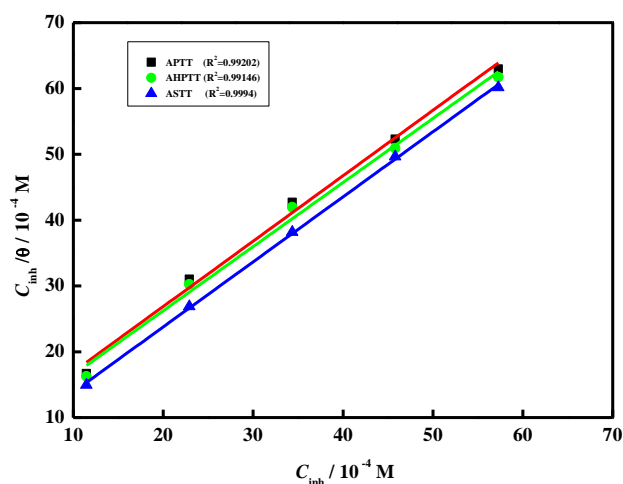


Figure 3. Langmuir adsorption isotherm plots for the adsorption of the triazoles derivatives on the mild steel surface in 1.0 M HCl solution

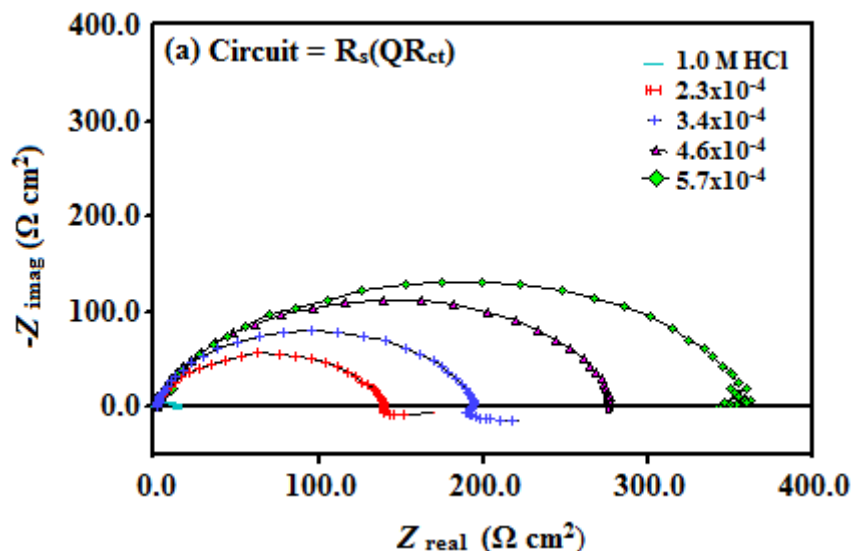
When it is around -40 kJ mol^{-1} or higher values it involve charge sharing or charge transfer from organic molecules to the metal surface to form a coordinate type of bond that is chemisorption [25, 26]. The calculated ΔG_{ads}^0 values range from -34.8 to $-36.2 \text{ kJ mol}^{-1}$ (Table 4). This indicates that triazoles are adsorbed chemically and physically on steel surface in 1.0 M HCl solution. The unshared electron pairs of heteroatom interact with d-orbital of iron atom of steel to provide a protective chemisorbed film [27].

3.3 Electrochemical measurements

3.3.1 Electrochemical impedance spectroscopy (EIS) studies

The corrosion behaviour of mild steel in 1.0 M HCl in the absence and presence of triazoles (APTT, AHPTT and ASTT) was investigated by EIS after immersion for 30 min at 308 K. Nyquist and Bode-phase plots of mild steel in uninhibited and inhibited acid solutions containing various concentrations of triazoles are presented in Fig. 4a-c and Fig. 5a-c. The impedance diagram (Nyquist) contain depressed semicircles with the center under real axis with one capacitive loop in the high frequency (HF) zone, and with 4-amino-5-(2-hydroxy) phenyl-4*H*-1, 2, 4,-triazole-3-thiol, (AHPTT) there is one inductive loop also in lower frequency (LF) zone. The HF semicircle is attributed to the time constant of charge transfer and double-layer capacitance [28, 29]. The LF inductive loop may be attributed to the relaxation process obtained by adsorption species as Cl_{ads}^- and H_{ads}^+ on the electrode surface [30, 31].

The capacitance is modelled by constant phase element (CPE) and the corresponding model of the interface by an equivalent circuit in Fig 4a-c. In case of APTT and ASTT this equivalent circuit, constant phase element (CPE) is parallel to the charge transfer resistance (R_{ct}), and for AHPTT CPE is parallel to the charge transfer resistance (R_{ct}), this is in series to the parallel of inductive elements (L) and R_{L} .



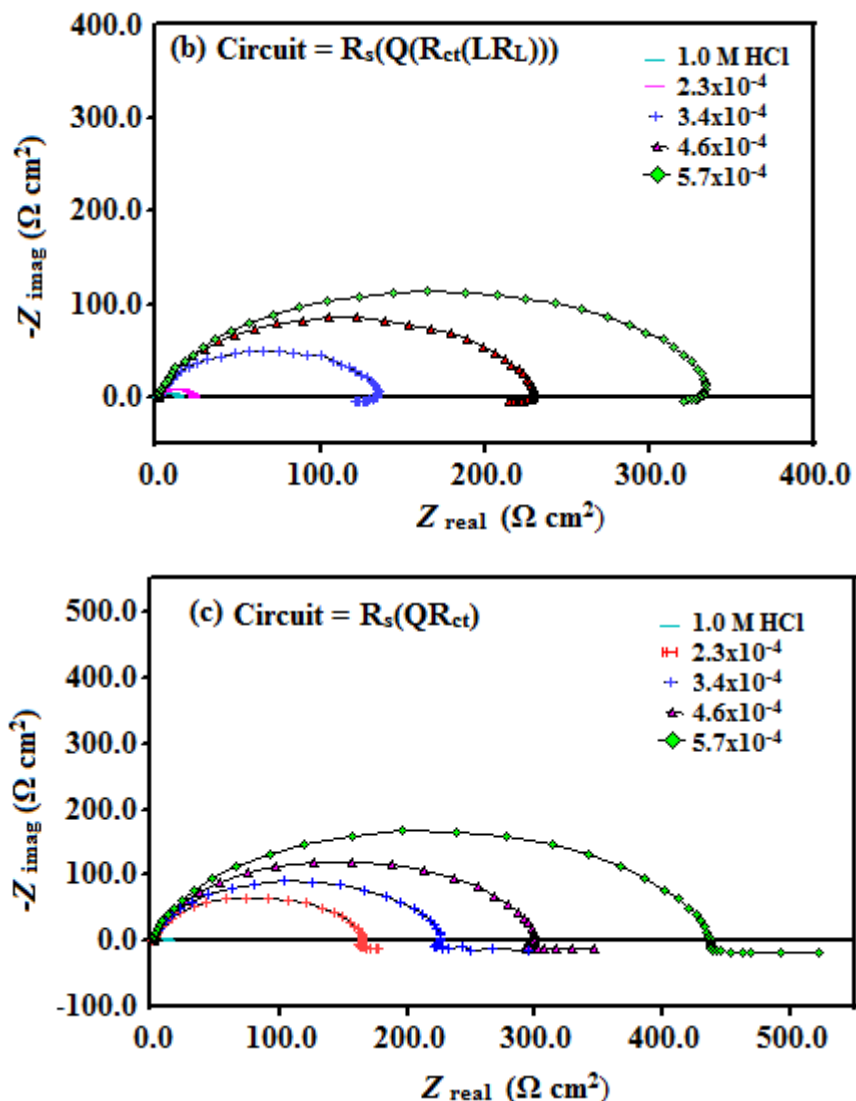


Figure 4. Nyquist plots for the mild steel in 1.0 M HCl containing different concentrations of (a) APTT, (b) AHPTT and (c) ASTT.

The CPE impedance is given by equation: [32].

$$Z_{CPE} = Y_0^{-1} (i\omega)^{-n} \tag{11}$$

where Y_0 is the CPE constant, ω is the angular frequency ($= 2\pi f_{max}$ in rad s^{-1}) and n is a CPE exponent which can be used as a gauge of the heterogeneity or roughness of the surface. The double layer capacitance values C_{dl} derived from the CPE parameters according to:

$$C_{dl} = (Y_0 R_{ct}^{1-n})^{1/n} \tag{12}$$

According to the above-mentioned equivalent circuit, experimental data were fitted very well. The impedance parameters are listed in Table 5. It can be seen from Table 5, that R_{ct} values increased with

increasing the concentration of the inhibitors, which suggesting that a charge transfer process mainly controlling the corrosion process. The change of R_{ct} and Y_0 values can be related to the gradual replacement of water molecules by inhibitor molecules from the surface which decreases the number of active sites necessary for corrosion reaction [33]. On the other hand the values of C_{dl} decreases with an increase in the inhibitor concentration. The double layer between the charged metal surface and the solution is considered as an electrical capacitor. The adsorption of inhibitors on the mild steel may be attributed to the formation of a protective layer on the surface [34].

The inhibition efficiency ($\eta_{\%}$) of the inhibitor was calculated by the charge transfer resistance values using the following equation:

$$\eta_{\%} = \frac{R_{ct}^i - R_{ct}^0}{R_{ct}^i} \times 100 \quad (13)$$

where, R_{ct}^0 and R_{ct}^i are the charge transfer resistance in absence and in the presence of inhibitor, respectively. Figs.5a-c presents Bode plots in the presence of different concentrations of inhibitor. From the Bode plots Figs.5a-c, there is no distinct diversification of impedance modulus, and the impedance modulus increase with inhibitor concentration. The continuous increase in the phase angle shift correlating with the increase of inhibitor adsorbed on mild steel surface.

3.3.2 Potentiodynamic polarization measurements

Polarization curves for mild steel at various concentrations of triazoles in aerated solutions are shown in Fig. 6a-c. It is clear from the potentiodynamic curves that the presence triazoles, in acid solution, decrease the corrosion rate. The decrease in I_{corr} value is due to the adsorption of the inhibitor molecules [35]. It is observed that both the cathodic and anodic reactions are suppressed with the addition of triazoles which suggest that all triazoles inhibit both anodic dissolution and cathodic hydrogen evolution reaction. Electrochemical corrosion parameters i.e. corrosion potential (E_{corr}), cathodic and corrosion current density (I_{corr}) obtained from the Tafel extrapolation of the polarization curves along with inhibition efficiency are given in Table 4. The inhibition efficiency ($\eta_{\%}$) was calculated using the following equation:

$$\eta_{\%} = \frac{I_{corr}^0 - I_{corr}^i}{I_{corr}^0} \times 100 \quad (14)$$

where, I_{corr}^0 and I_{corr}^i are the corrosion current density in absence and in the presence of inhibitor, respectively. There was no significant change in the E_{corr} values in the presence of triazoles which suggest that triazoles are mixed type inhibitors [36, 37].

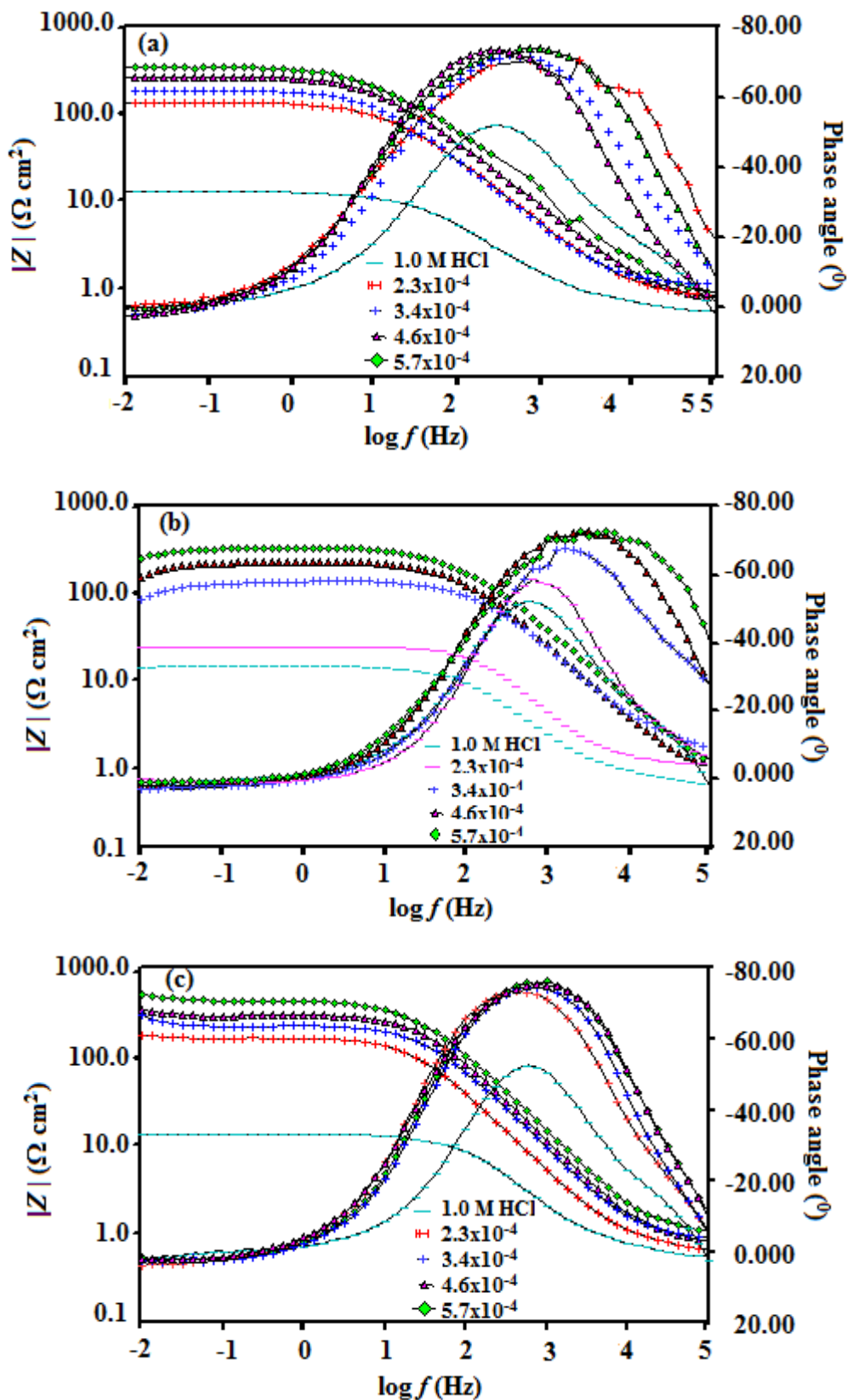
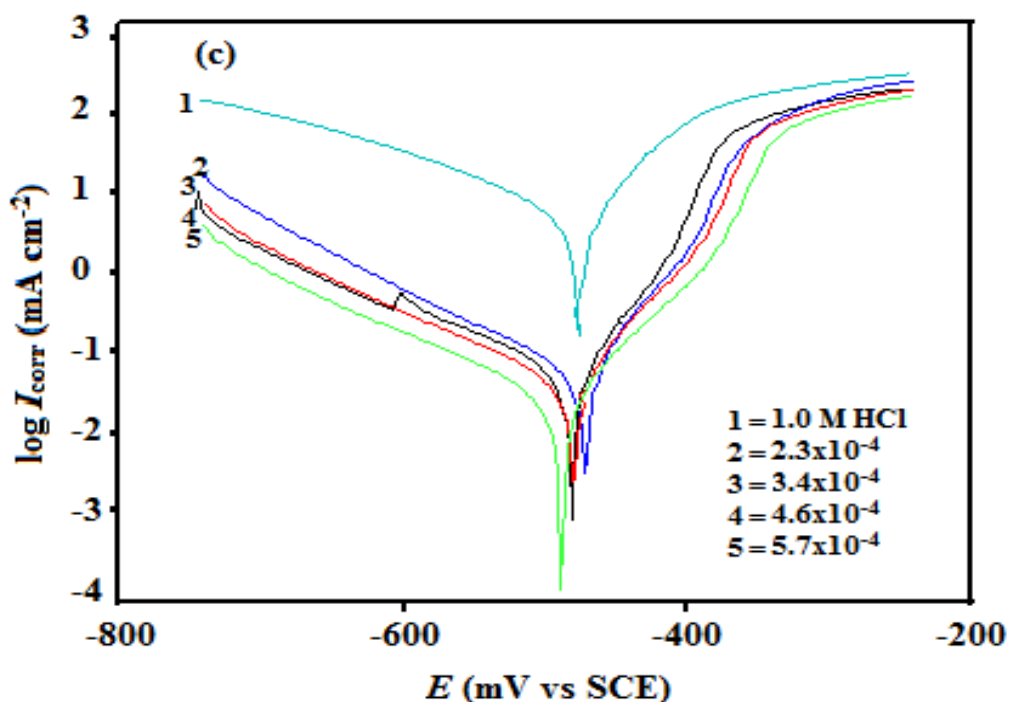


Figure 5. Bode plots of mild steel in absence and presence of different concentrations for (a) APTT, (b) AHPTT and (c) ASTT in 1.0 M HCl.

Table 5. Calculated electrochemical parameters for mild steel in absence and presence of different concentrations of different inhibitors

Conc. of inhibitor (mol L-1)	Parameters							
	Rs (Ω)	Q Yo (μF cm-2)	n	Rct (Ω cm2)	L/H	RL (Ω cm2)	Cdl (μF cm-2)	(η%)
1.0 M HCl	0.580	482.0	0.789	12.98	-	-	124.08	-
APTT								
2.29 x 10-4	0.826	49.74	0.884	137.5	-	-	25.85	90.54
3.43 x 10-4	1.154	43.93	0.907	196.6	-	-	26.98	93.40
4.58 x 10-4	0.711	31.44	0.887	269.9	-	-	17.12	95.19
5.72 x 10-4	0.711	30.20	0.854	328.5	-	-	13.72	96.04
AHPTT								
2.29 x 10-4		130.00	0.875	21.21	-0.257	-0.892	56.01	38.80
3.43 x 10-4	0.944	31.10	0.831	96.65	107.4	34.14	9.55	86.57
4.58 x 10-4	1.220	21.73	0.866	183.0	138.5	40.85	9.23	92.90
5.72 x 10-4	0.716	19.49	0.834	282.4	169.2	42.24	6.92	95.40
ASTT								
2.29 x 10-4		84.70	0.883	165.3	-	-	48.11	92.15
3.43 x 10-4	0.693	42.60	0.897	227.3	-	-	25.01	94.29
4.58 x 10-4	0.910	34.97	0.897	299.5	-	-	20.67	95.67
5.72 x 10-4	0.825	30.28	0.885	437.2	-	-	17.21	97.03
	1.035							



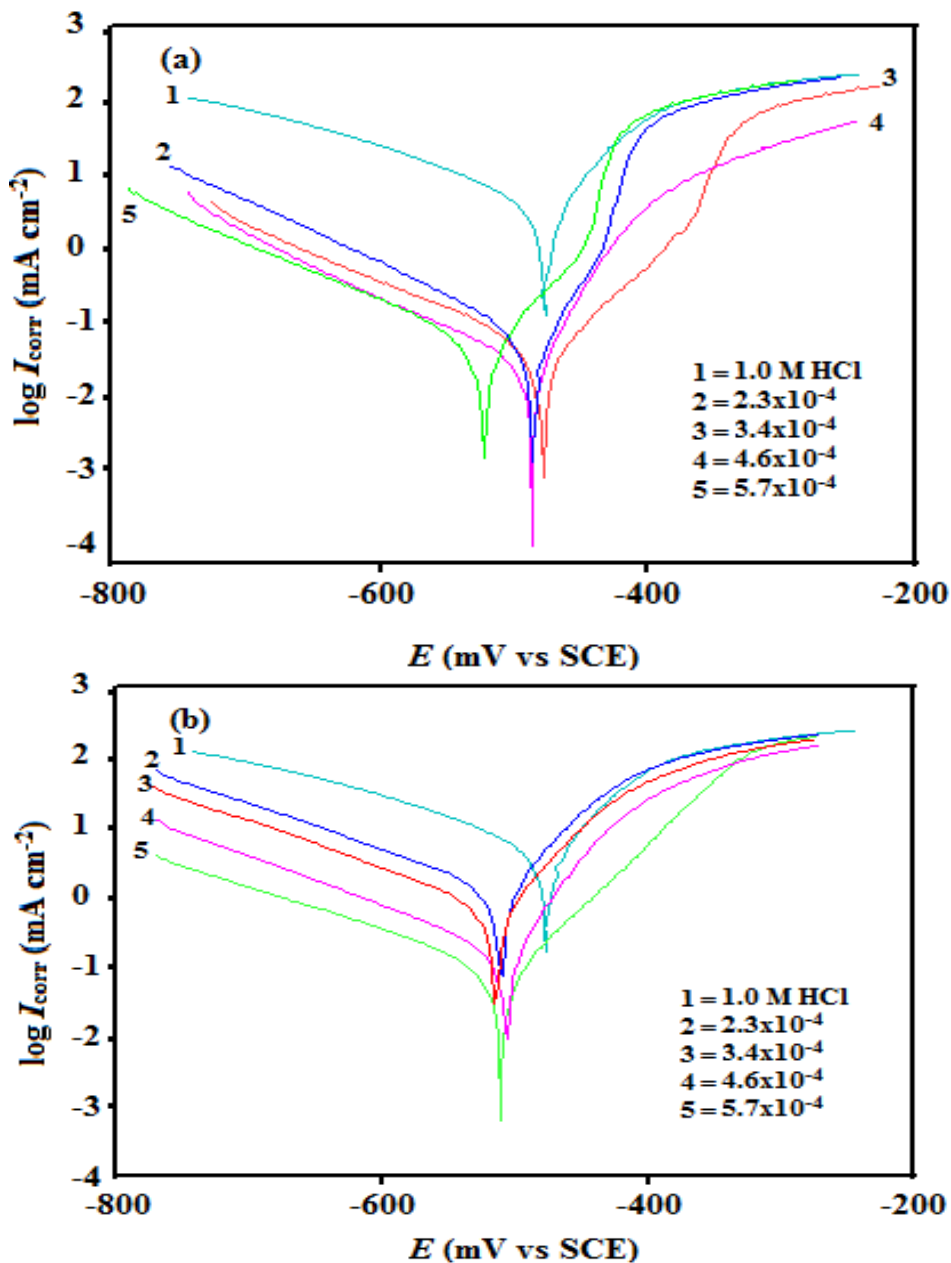


Figure 6. Polarization curves for corrosion of mild steel in 1.0 M HCl in the absence and presence of different concentrations of (a) APTT, (b) AHPTT and (c) ASTT.

3.3.3 Linear polarization resistance

In LPR measurements, polarization resistance values are derived from the slope of the potential-current density ($\Delta E/\Delta I$) curve. From the calculated polarization resistance value, the inhibition efficiency ($\eta_{\%}$) was calculated using the relationship:

$$\eta_{\%} = \frac{R_p^i - R_p^0}{R_p^i} \times 100 \tag{15}$$

where, R_p^0 and R_p^i are the polarization resistance in absence and in the presence of inhibitors, respectively. The R_p values in absence and presence of inhibitors are given in table 6. Table 6 it is seen that R_p values increase in presence of triazoles which suggest inhibition of mild steel corrosion [38, 39].

Table 6. Polarization parameters for mild steel in 1.0 M HCl in the absence and presence of triazoles derivatives at different concentrations.

Conc. of inhibitor	Tafel polarization data			Linear polarization data	
	E_{corr} (mV vs. SCE)	I_{corr} ($\mu\text{A cm}^{-2}$)	Inhibition efficiency ($\eta\%$)	R_p ($\Omega \text{ cm}^2$)	Inhibition efficiency ($\eta\%$)
1.0 M HCl	-477.00	1780	-	18.20	-
APTT					
2.29 x 10 ⁻⁴	-479.0	61.50	96.54	125.7	85.52
3.43 x 10 ⁻⁴	-488.0	48.80	97.26	177.7	89.75
4.58 x 10 ⁻⁴	-486.0	42.00	97.64	245.5	92.59
5.72 x 10 ⁻⁴	-523.0	35.10	98.02	320.6	94.32
AHPTT					
2.29 x 10 ⁻⁴	-516.0	997.0	95.11	24.78	26.55
3.43 x 10 ⁻⁴	-508.0	190.0	95.99	80.98	77.52
4.58 x 10 ⁻⁴	-512.0	55.70	90.54	169.1	89.24
5.72 x 10 ⁻⁴	-511.0	39.50	97.78	261.8	93.05
ASTT					
2.29 x 10 ⁻⁴	-472.0	66.60	96.26	180.0	89.89
3.43 x 10 ⁻⁴	-481.0	58.00	96.74	325.3	94.40
4.58 x 10 ⁻⁴	-482.0	51.60	97.10	330.8	94.49
5.72 x 10 ⁻⁴	-491.0	31.90	98.21	512.1	96.45

4. CONCLUSIONS

- (i) All the triazoles namely 4-amino-5-phenyl-4*H*-1, 2, 4,-triazole-3-thiol (APTT), 4 - amino-5-(2-hydroxy) phenyl-4*H*-1, 2, 4,-triazole-3-thiol, (AHPTT), 4-amino-5-styryl-4*H*-1, 2, 4,-triazole-3-thiol, (ASTT) were found to inhibit the corrosion of mild steel in 1.0 M HCl solution.
- (ii) The order of inhibition efficiency for triazoles was as follows ASTT > AHPTT > APTT.
- (iii) ASTT showed highest inhibition efficiency of 98.21 % at concentration of 5.72 x 10⁻⁴ mol L⁻¹.

- (iv) The study of EIS showed that all the triazoles studied inhibit corrosion by adsorption mechanism.
- (v) The adsorption of triazoles on mild steel surface is found to obey the Langmuir adsorption isotherm and they are mixed-type inhibitors.

ACKNOWLEDGEMENT

Authors acknowledge financial support from University Grant Commission (UGC), New Delhi, India Project F No. 40-101/2011(SR) UGC.

References

1. G. Schmitt, *Brit. Corros. J.* 19 (1984) 165
2. V.S. Sastri and J.R. Perumareddi, *Corrosion* 53 (1997) 617
3. H.H. Hasan, E. Abdelghani and M.A. Amin, *Electrochim. Acta.* 52 (2007) 6359
4. D. K. Yadav, B. Maiti and M. A. Quraishi, *Corros. Sci.* 52 (2010) 3586
5. M. Lagrene, B. Mernari, M. Bouanis, M. Traisnel and F. Bentiss, *Corros. Sci.* 44 (2002) 573
6. A. K. Singh, M. A. Quraishi and E. E. Ebenso, *Int. J. Electrochem. Sci.* 6 (2011) 5673
7. M. Ashok and B.S. Holla, *J. Pharmacol. Toxicol.* 2 (2007) 256
8. M.C. Hosur, M.B. Talwar, R.S. Bennur, S.C. Benur, P.A. Patil and S. Sambrekar, *Indian J. Pharm. Sci.* 55 (1993) 86
9. B.S. Holla, B. Veerendra, M.K. Shivananda and B. Poojary, *Eur. J. Med. Chem.* 38, (2003) 759
10. D.J. Prasad, M. Ashok, P. Karegoudar, B. Poojary, B.S. Holla and K.N. Sucheta, *Eur. J. Med. Chem.* 44, (2009) 551
11. M. Finsgar and I. Milosev, *Corros. Sci.* 52 (2010) 2737
12. E.M. Sherif and Su-M. Park, *Electrochim. Acta.* 51 (2006) 4665
13. M.A. Amin, S.S. Abd El-Rehim, E.E.F. El-Sherbini and R.S. Bayyomi, *Electrochim. Acta* 52 (2007) 3588
14. A.M.S. Abdennaby, A.I. Abdulhadi, S.T. Abu-Orabi and H. Saricimen, *Corros. Sci.* 38 (1996) 1791
15. S.K. Shukla, A.K. Singh, I. Ahamad and M.A. Quraishi, *Mater. Lett.* 63 (2009) 819
16. (a) P. K. Sahoo, R.Sharma and P. Pattanayak, *Med. Chem. Res.* 19 (2010) 127 (b)K.S Dhaka, J. Mohan, V.K. Chadha and H.K. Pujari, *Indian J. Chem.* 12 (1974) 28
17. I. Ahamad, R. Prasad and M.A. Quraishi, *Corros. Sci.* 52 (2010) 3033.
18. A. K. Singh and M. A. Quraishi, *J. Appl. Electrochem.* 41 (2011) 7
19. A. K. Singh and M. A. Quraishi, *Corros. Sci.* 53 (2011) 1288
20. N.P. Clark, E. Jakson and M. Robinson, *Br. Corros. J.* 14 (1979) 33
21. D. K. Yadav, M. A. Quraishi and B. Maiti, *Corros. Sci.* 55 (2012) 254
22. E. S. Ferreira, C. Giancomelli, F. C. Giacomelli and A. Spinelli, *Mater. Chem. Phys.* 83 (2004) 129
23. B. Donnely, T.C. Downie, R. Grzeskowiak, H.R. Hamburg and D. Short, *Corros. Sci.* 18 (1978) 109
24. G. Avci, *Mater. Chem. Phys.* 112 (2008) 234
25. A. Yurt, A. Balaban, S. Ustün Kandemir, G. Bereket and B. Erk, *Mater. Chem. Phys.* 85 (2004) 420
26. A. K. Singh and M. A. Quraishi, *Corros. Sci.* 52 (2010) 1373
27. A. K. Singh and M. A. Quraishi, *Corros. Sci.* 52 (2010) 1529
28. C. Deslouis, B. Tribollet, G. Mengoli and M. M. Musiani, *J. Appl. Electrochem.* 18 (1988) 374
29. S. S. Abdel Rehim, H. H. Hassan and M. A. Amin, *Appl. Surf. Sci.*, 187 (2002) 279

30. A. Sorkhabi, D. Seifzadeh and M. G. Hosseini, *Corros. Sci.* 50 (2008) 3363
31. M.A. Amin, K.F. Khaled, Q. Mohsen and H.A. Arida, *Corros. Sci.* 52 (2010) 1684
32. R.A. Bustamante, G.N. Silve, M.A. Quijano, H.H. Hernandez and M.R. Romo, *Electrochim. Acta.* 54 (2009) 5393
33. Cuan and M.P. Pardave, *Electrochim. Acta.* 54 (2009) 5393
34. S. Zhang, Z. Tao, W. Li and B. Hou, *Appl. Surf. Sci.* 255 (2009) 6757
35. K.F. Khaled and M.A. Amin *Corros. Sci.* 51 (2009) 1964
36. M.A. Quraishi, M.Z.A. Rafiquee, S. Khan and N. Saxena, *J. Appl. Electrochem.* 37 (2007) 1153
37. I. Ahamad, R. Prasad and M.A. Quraishi, *J. Solid State Electrochem.* 14 (2010) 2095
38. A.K. Singh and M. A. Quraishi, *Corros. Sci.* 51 (2009) 2752
39. S. K. Shukla and M.A. Quraishi, *J. Appl. Electrochem.* 39 (2009) 1517